



# CLOSED FORM SOLUTIONS FOR THE POINT MOBILITIES OF AXISYMMETRICALLY EXCITED CYLINDRICAL SHELLS

O. FÉGEANT

*Department of Building Sciences, Royal Institute of Technology (KTH), SE-100 44 Stockholm, Sweden.*

*E-mail: olivier@bim.kth.se*

*(Received 21 February 2000, and in final form 4 September 2000)*

Closed form formulae are reported describing point mobilities for thin cylindrical shells in axisymmetric motion. Two cases are studied: (1) the infinite shell and (2) the edge-excited semi-infinite shell and, for both, forces and moment excitation are considered. The solutions of these problems are obtained analytically by resorting to perturbation methods and presented in terms of the Green functions and point mobilities. These results are further used to derive approximate expressions for the reflection coefficients of the shell-borne waves at a free end and for the Green functions of a finite free-free shell undergoing axisymmetric vibrations.

© 2001 Academic Press

## 1. INTRODUCTION

Point mobility for a mechanical system is defined as the complex ratio of velocity to force during harmonic motion. In mechanical engineering, this concept is widely used for studying the vibration transmission to structures by force and moment. Formulae describing mobilities of infinite and semi-infinite simple structural elements such as beams, plates and shells are desirable from the theoretical point of view. Indeed, analytical solutions display explicitly the functional dependence of the solutions on the problem parameters, thus yielding a physical insight into the underlying mechanisms which govern the structure response. Their benefit is, however, not limited to theoretical considerations and they also find application in practice. For instance, design methods based upon substructuring techniques (see, e.g., references [1, 2]), resort to such formulae to study the vibration transmission in built-up structures. A further application is that they provide estimates for the vibration levels of similar but finite structures [3].

Mobilities of beams and plates having infinite or semi-infinite extent have been the focus of a vast number of past, as well as recent, studies (see, e.g., references [3–6]), yielding closed-form solutions for a number of problems. For shells, the results reported by the literature are fewer and have been obtained mainly numerically (see, e.g., references [7–10]). In fact, scant attention has been devoted to the derivation of analytical solutions, perhaps due to the complexity of the differential equations governing shell motions. The first to attempt to fill this void was Franken in 1960 [11]. Neglecting the flexural stiffness of the shell, he derived an analytical expression for the mobility of an infinite thin-walled shell with respect to a radial point force. Addressing the same problem 2 years later, Heckl [12] obtained approximate solutions including the flexural stiffness. It can be pointed out that, by taking advantage of the infinite character of the structure, both studies resort to the

method of residues. Regarding the case of semi-infinite shell subject to loads applied at its end, the static case was solved explicitly by Simmonds in 1966 [13]. Recently, Ming *et al.* [10] have presented numerical results for the dynamical version of this problem. However, no attempt has been made to derive closed form solutions of the mobilities of semi-infinite shells. This may be due to the fact that the method of residues cannot be used with equal success to deal with semi-infinite structures as shown in references [5, 6].

With consideration of only the axisymmetric mode of vibration, the present paper reports on closed form formulae describing point mobilities for thin-walled cylindrical shells of infinite and semi-infinite extent. The formulae are given for three types of load, namely an axial force, a radial force and a bending moment. Regarding the infinite shell problem, the present results complete those obtained by Franken [11] and Heckl [12] in the case of radial excitation. Further, since being a stage in the derivation of the mobilities, approximate expressions for the shell Green functions are also presented. The validity of the present results is bounded by the limitations inherent in the following assumptions: (1) Love's first approximation [14], (2) vibrations *in vacuo*, and (3) point excitation in the axial direction, i.e., the size of the excitation in this direction is larger than the shell thickness but small compared to the axial wavelength.

The theoretical approach adopted in this study is based upon perturbation methods. This strategy was used successfully by Wong *et al.* [15] to derive the normal frequencies of a clamped cylindrical shell vibrating axisymmetrically. The problems addressed here are formulated using the theory by Flügge [16] and solved analytically by applying the method of the matched asymptotic expansions [17]. Solutions are obtained in the form of power-series expansions with the thickness-to-radius ratio of the shell taken as expansion parameter. Retaining the leading terms of these expansions yields approximate expressions of the shell Green functions with respect to the different loads. Finally, the analysis is pursued to higher order terms in order to obtain expressions for both the real and the imaginary parts of the point mobilities.

The plan of this paper is as follows. Section 2 is concerned with the problem formulation and presents the methodology for the computerisation of the results. In section 3, the equations are re-written in line with perturbation theory and solved for the leading term to exemplify the method. It appears that the derived expressions exhibit a singularity slightly below the first ring frequency. In section 4, the Green functions and the mobilities of the semi-infinite and infinite shells with respect to the different loads are given in closed form and are shown to compare well with exact calculations. Section 5 deals with the singularities appearing in the previous results. They are tackled by resorting again to perturbation theory and the derived results are represented by formulae containing tabulated functions. Finally, section 6 provides approximate expressions for the reflection coefficients of the shell-borne waves at a free end and for the response of a finite free-free cylindrical shell.

## 2. PROBLEM FORMULATION

The mechanical response of a cylindrical shell to an axisymmetric load is addressed for the three following problems: the case of the semi-infinite shell excited at its end (problem I); the case of the infinite shell excited in its middle (problem II) and the case of the free-free finite shell (problem III). Problems I and II can be tackled by studying a semi-infinite shell with certain sets of boundary conditions while solutions for problem III are derived from results of the two former problems.

## 2.1. GOVERNING EQUATIONS

Let a thin circular semi-infinite shell made of a homogeneous isotropic material vibrate *in vacuo* in its axisymmetric mode. The shell occupies the half-space  $x > 0$  (see Figure 1) and, according to Flügge shell theory [16], its displacements in the axial and radial directions, respectively, denoted  $u$  and  $w$ , are governed by the two differential equations

$$u'' + \Omega^2 u + \mu w' - \beta w''' = 0, \quad \mu u' - \beta u'' + (1 - \Omega^2)w + \beta(w + w^{(4)}) = 0, \quad (1)$$

where  $\mu$  is the Poisson ratio,  $\beta$  the thickness parameter and  $\Omega$  the non-dimensional frequency. The reader is referred to the nomenclature given in Appendix B for the definition of parameters not explicitly given in the text. Primes denote differentiation with respect to the non-dimensional axial length  $s = x/R$  and derivatives of order  $n$  higher than 3 are denoted  $\partial^n(\cdot)/\partial s^n = (\cdot)^{(n)}$  to lighten the equations. In order to make the present analysis more convenient, equation (1) is rearranged in the form

$$\begin{aligned} \beta(1 - \beta)w^{(6)} + \beta(\Omega^2 + 2\mu)w^{(4)} + (\beta + 4m^4)w'' + \Omega^2(1 - \Omega^2 + \beta)w &= 0, \\ (\mu + \Omega^2\beta)u' &= -((1 - \Omega^2 + \beta)w + \mu\beta w'' + \beta(1 - \beta)w^{(4)}), \end{aligned} \quad (2a,b)$$

where the notation

$$4m^4 = 1 - \mu^2 - \Omega^2 \quad (3)$$

has been introduced.

Free axisymmetric vibrations of semi-infinite shells can be expressed in terms of three waves of propagating or nearfield types. Upon omitting the time dependence  $e^{i\omega t}$ , its general form may be taken as

$$\begin{Bmatrix} w \\ u \end{Bmatrix} = \begin{Bmatrix} C_1 \\ A_1 \end{Bmatrix} e^{\kappa_1 s} + \begin{Bmatrix} C_2 \\ A_2 \end{Bmatrix} e^{\kappa_2 s} + \begin{Bmatrix} C_3 \\ A_3 \end{Bmatrix} e^{\kappa_3 s}, \quad (4)$$

where  $\kappa_p$ ,  $C_p$  and  $A_p$  are the non-dimensional propagation constant, the amplitude in the radial and the axial directions of the wave  $p$  ( $p = 1, 2, 3$ ) respectively.

Substituting the form of solutions (4) into equation (2a) leads to a sixth order polynomial in  $\kappa_p$ , also termed the dispersion relation. The three propagation constants are the roots of the dispersion relation which yield solutions satisfying Sommerfeld's condition in the half-space  $x > 0$ . Accordingly, and owing to the time dependence adopted, these constants are the roots located in the complex half-plane described by  $\pi/2 < \arg(\kappa) \leq 3\pi/2$ . Further, to each wave  $p$  ( $p = 1, 2, 3$ ) is associated a wave amplitude ratio, denoted  $T_p = A_p/C_p$ , and which expression is easily obtained by introducing equation (4) in equation (2b).

In both problems I and II, the shell is submitted to an axisymmetric excitation at  $x = 0$ . The excitation consists of an axial force, a radial force and a bending moment. The distributions of these loads per unit length are  $(N_0, Q_0, M_0)$  and the convention which is employed regarding their positive directions is shown in Figure 1. Problem II (infinite shell) is transformed into a boundary-value problem by considering the response of a semi-infinite shell and a set of boundary conditions at  $x = 0$  in accord with the symmetry of the infinite shell. For problem I, i.e., the semi-infinite shell excited at the edge, the set of boundary conditions reads [16]

$$\begin{aligned} (4m^4 w + \beta(w + w^{(4)} + \mu w'' - u'''))/\mu|_{s=0} &= n_0, \\ (w''' - u'')|_{s=0} &= q_0, \quad (w'' - u')|_{s=0} = m_0. \end{aligned} \quad (5a-c)$$

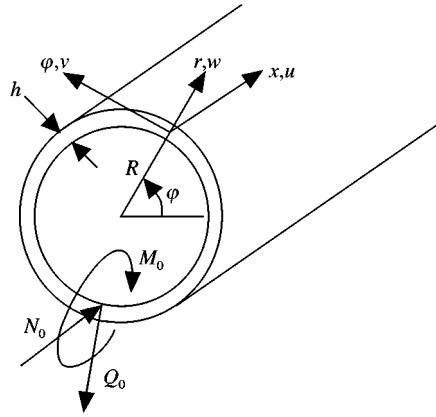


Figure 1. Geometry of the semi-infinite shell, co-ordinate system and positive convention of force and moment resultants.

The right-hand members of equation (5) are defined by

$$n_0 = RN_0/B, \quad q_0 = R^3Q_0/D, \quad m_0 = -R^2M_0/D, \tag{6}$$

where  $B = Eh/(1 - \mu^2)$  and  $D = Eh^3/12(1 - \mu^2)$  are the extensional and the flexural rigidities respectively. In Flügge’s theory, the boundary condition with respect to the axial force is usually given in the form

$$(u' + \mu w - \beta w'')|_{s=0} = -n_0, \tag{7}$$

instead of equation (5a). Equation (5a) is obtained by re-arranging equation (7) together with equation (1b) and was derived in order to save some algebra in the future analysis.

For problem II, i.e., the case of the infinite shell excited in its “middle”, symmetry implies that half of the exciting load acts on each half of the shell. Furthermore, two sets of boundary conditions have to be considered. One deals with the excitation by a radial force and reads

$$u|_{s=0} = 0, \quad w|_{s=0} = 0, \quad (w''' - u'')|_{s=0} = q_0/2, \tag{8}$$

while the second deals with axial force excitation and bending moment excitation:

$$(4m^4w + \beta(w + w^{(4)} + \mu w'' - u'''))/\mu|_{s=0} = n_0/2, \tag{9}$$

$$(w'' - u')|_{s=0} = m_0/2, \quad w|_{s=0} = 0.$$

## 2.2. SOLUTIONS TO THE BOUNDARY-VALUE PROBLEMS

To determine the response of the shell, the dispersion relation is solved to find the three propagation constants satisfying Sommerfeld’s condition and the associated wave amplitude ratios  $T_p$  are calculated. Then, substituting the displacement equations (4) into the boundary conditions given by either equation (5), equation (8) or equation (9) and using the previously calculated  $T_p$  and  $\kappa_p$  yield a system of three equations with the wave amplitudes  $C_1, C_2$  and  $C_3$  as unknowns. Solving this system to find these constants gives the receptances of each wave to the different loads. Written in matrix form, the amplitudes of the waves are given by

$$\mathbf{C} = \boldsymbol{\alpha}^c \mathbf{X}, \tag{10}$$

where  $\mathbf{C} = [C_1 \ C_2 \ C_3]^T$  and  $\mathbf{X} = [N_0 \ Q_0 \ M_0]^T$ . The matrix  $\alpha^c$  is referred to as the wave receptance matrix. The element  $\alpha_{p,X}^c$  is the receptance of the wave  $p$  with respect to the load  $X$  ( $X = N_0, Q_0, M_0$ ). The superscript  $c$  is either  $c = \infty/2$  or  $\infty$  depending on whether reference is made to problem I (semi-infinite shell) or II (infinite shell).

Once the receptances of the waves are known, the direct mobilities, which are defined as the complex ratio of velocity to force taken at the same point, are easily derived. For the sake of convenience, they are gathered in matrix form as follows:

$$[\dot{u} \ \dot{w} \ \dot{\theta}]^T = \mathbf{Y}^c \mathbf{X}. \quad (11)$$

The overdot denotes time derivation and  $\theta$  represents the rotation of the normal to the middle surface about the  $\varphi$ -axis,  $\theta = \partial w / \partial x$ . The mobility matrix is symmetric and reads explicitly

$$\mathbf{Y}^c = \begin{bmatrix} Y_{u,N_0}^c & Y_{u,Q_0}^c & Y_{u,M_0}^c \\ Y_{w,N_0}^c & Y_{w,Q_0}^c & Y_{w,M_0}^c \\ Y_{\theta,N_0}^c & Y_{\theta,Q_0}^c & Y_{\theta,M_0}^c \end{bmatrix}. \quad (12)$$

Diagonal and off-diagonal terms are referred to as input and cross-mobilities respectively. They are related to the wave receptances by the relationships

$$Y_{u,X}^c = i\omega \sum_{p=1}^3 T_p \alpha_{p,X}^c, \quad Y_{w,X}^c = i\omega \sum_{p=1}^3 \alpha_{p,X}^c, \quad Y_{\theta,X}^c = i\omega \left( \sum_{p=1}^3 \alpha_{p,X}^c k_p \right) / R. \quad (13a-c)$$

For single force or moment excitation, the power injected into the shell is proportional to the real part of the input mobility. In case of joint excitation, i.e., excitation consisting of several components (forces, moments) correlated in time, cross-mobilities should be taken into consideration when calculating the injected power. Unlike input mobilities, the sign of the real part of the cross-mobilities may change, reflecting the possible reduction of power input by a certain combination of loads at the end of the structure.

### 3. THE PERTURBATION APPROACH

For thin shells the thickness parameter, which is proportional to the square of the thickness-to-radius ratio, is very small ( $\beta \ll 1$ ). Equation (2a) shows that this small parameter multiplies the highest derivative of the differential equation. This form of differential equation is typical of *edge-layer* problems for which the variable of the problem undergoes rapid changes across a narrow region [17]; the term *edge-layer* refers to the fact that these regions frequently adjoin the boundary of the system. However, such layers should also be expected in the narrow regions adjoining load application points or discontinuities in the structure.

Setting  $\beta = 0$  in equation (2) yields the well-known membrane equation for shells. Using membrane theory for studying the axisymmetric vibrations of shells is valid as long as the edge layer can be neglected, i.e., at some distance from the boundary and at low frequencies. The membrane equation being of second order, the vibration field is modelled by only one wave and fails to satisfy the three boundary conditions at the edge. The two boundary conditions involving bending stresses, i.e., the ones on the radial force and the bending moment, should be dropped. However, for infinite shell membranes, transverse shear stresses are balanced by extensional stresses and the membrane theory can be used to assess

the receptance of the shell to a radial force at low frequencies [11]. Conversely, the membrane theory is inadequate to predict the response of a semi-infinite shell to a radial load located at its edge as the extensional stresses vanish there.

Among the perturbation methods, a most effective technique for treating edge-layer problems is the method of the matched asymptotic expansions [17]. This method divides the structure into an inner region adjoining the boundary and an outer region including the rest of the structure. The sharp changes taking place in the inner region are described using a magnified scale. The governing equations and the boundary conditions are expressed in the new co-ordinate system and expanded as a function of the thickness parameter. The displacement vector expansion, the solution of these equations, is referred to as the inner solution. In the outer region, the equations of motion are expanded by using the original co-ordinate system. The solution of these equations is called the outer solution. The basic idea underlying the method is that the domains of validity of the two expansions overlap and hence their matching provides the additional equations which allow all the constants in the expansions to be determined. Finally, the inner and outer expansions are combined to form a composite expansion valid both in the inner and outer regions. In the following section, the governing equations and the boundary conditions for problem I (semi-infinite shell) are re-arranged according to the method. Thereafter, the derivation of the wave receptances is exemplified by determining the solutions at the leading order. However, it proved necessary to extend the analysis to higher orders in order to obtain approximate expressions for all the wave receptances. The results of this further analysis are presented for both the semi-infinite and infinite shells in section 4.

### 3.1. GOVERNING EQUATIONS IN THE INNER REGION

Following references [15, 17], the inner solutions, denoted  $u^i$  and  $w^i$ , are sought in the form

$$u^i = \sum_{k=0}^{\infty} \lambda^k \tilde{u}_k, \quad w^i = \sum_{k=0}^{\infty} \lambda^k \tilde{w}_k, \quad (14)$$

where the expansion parameter is chosen to be

$$\lambda = \beta^{1/4}. \quad (15)$$

Accordingly, modified sets of governing equations and boundary conditions are derived by applying the stretching transformation  $\xi = s/\lambda$  to equations (2) and (5). Introducing equation (14) in the modified equations of motion and collecting by terms of equal power of  $\lambda$  yields

$$\begin{aligned} \tilde{w}_k^{(6)} + 4m^4 \tilde{w}_k'' &= -((\Omega^2 + 2\mu)\tilde{w}_{k-2}^{(4)} + \Omega^2(1 - \Omega^2)\tilde{w}_{k-2} + \tilde{w}_{k-4}'' - \tilde{w}_{k-4}^{(6)} + \Omega^2\tilde{w}_{k-6}), \\ \tilde{u}_k' &= -(1/\mu)((1 - \Omega^2)\tilde{w}_{k-1} + \tilde{w}_{k-1}^{(4)} + \mu\tilde{w}_{k-3}'' + \Omega^2\tilde{u}_{k-4}' + \tilde{w}_{k-5} - \tilde{w}_{k-5}^{(4)}), \end{aligned} \quad (16)$$

where the convention that  $\tilde{u}_k = \tilde{w}_k = 0$  for  $k < 0$  is adopted. Acting similarly with the modified boundary conditions for problem (I) yields

$$\begin{aligned} (4m^4 \tilde{w}_k + \tilde{w}_k^{(4)} + \mu\tilde{w}_{k-2}'' + \tilde{w}_{k-4} - \tilde{u}_{k-1}''')\mu^{-1}|_{\xi=0} &= \tilde{n}_0 \delta(k, 0), \\ (\tilde{w}_k''' - \tilde{u}_{k-1}'')|_{\xi=0} = \tilde{q}_0 \delta(k, 0) \quad (\tilde{w}_k'' - \tilde{u}_{k-1}')|_{\xi=0} &= \tilde{m}_0 \delta(k, 0), \end{aligned} \quad (17)$$

where  $\delta$  is Kronecker's delta function ( $\delta(k, 0) = 1$  if  $k = 0$ , 0 otherwise) and

$$\tilde{n}_0 = n_0, \quad \tilde{q}_0 = \lambda^3 q_0, \quad \tilde{m}_0 = \lambda^2 m_0. \quad (18)$$

### 3.2. GOVERNING EQUATIONS IN THE OUTER REGION

In the outer region, the solutions for the longitudinal and the radial displacements are denoted  $u^o$  and  $w^o$ . The solutions are sought in the form of

$$u^o = \sum_{k=0}^{\infty} \lambda^k \hat{u}_k, \quad w^o = \sum_{k=0}^{\infty} \lambda^k \hat{w}_k. \quad (19)$$

The equations satisfied by the functions  $\hat{u}_k$  and  $\hat{w}_k$  are derived by inserting equation (19) into equation (2) and collecting by terms of equal power of  $\lambda$ . This yields

$$4m^4 \hat{w}_k'' + \Omega^2(1 - \Omega^2) \hat{w}_k = -(\Omega^2 \hat{w}_{k-4} + \hat{w}_{k-4}'' + \hat{w}_{k-4}^{(6)} + (\Omega^2 + 2\mu) \hat{w}_{k-4}^{(4)} - \hat{w}_{k-8}^{(6)}),$$

$$\hat{u}_k' = -((1 - \Omega^2) \hat{w}_k + \Omega^2 \hat{u}_{k-4}' + \hat{w}_{k-4} + \mu w_{k-4}'' + \hat{w}_{k-4}^{(4)} - \hat{w}_{k-8}^{(4)})/\mu, \quad (20)$$

where the convention that  $\hat{u}_k = \hat{w}_k = 0$  for  $k < 0$  is adopted. It appears that up to and including the third order, these equations reduce to the membrane equation. For higher order, a non-homogeneous term appears, leading to particular solutions.

### 3.3. LEADING ORDER SOLUTIONS

The derivation of the wave receptances is exemplified for the leading order  $k = 0$ , i.e., the leading terms of the inner and outer expansions, are sought which satisfy both the boundary conditions and the matching equations. These solutions are then combined to form a composite expansion valid everywhere, thereby yielding the first approximation for the wave receptances.

At the leading order, i.e.,  $k = 0$ , the differential equations governing the vibrations in the inner region and given by equation (16) read

$$\tilde{w}_0^{(6)} + 4m^4 \tilde{w}_0'' = 0, \quad \tilde{u}_0' = 0 \quad (21)$$

and their solutions are

$$\tilde{w}_0 = C_{0,0}^1 + C_{0,1}^1 \xi + C_{0,0}^2 e^{-m(1+i)\xi} + C_{0,0}^3 e^{-m(1-i)\xi}, \quad \tilde{u}_0 = A_{0,0}^1. \quad (22)$$

Likewise at the leading order, equation (20) becomes

$$4m^4 \hat{w}_0'' + \Omega^2(1 - \Omega^2) \hat{w}_0 = 0, \quad \hat{u}_0' = -((1 - \Omega^2) \hat{w}_0)/\mu \quad (23)$$

and the outer solutions read

$$\hat{w}_0 = d_0 e^{-(\Omega\sqrt{\Omega^2 - 1/2m^2})s}, \quad \hat{u}_0 = -\frac{2m^2\sqrt{\Omega^2 - 1}}{\mu\Omega} d_0 e^{-(\Omega\sqrt{\Omega^2 - 1/2m^2})s} + b_0. \quad (24)$$

It is seen that the propagation constants not satisfying  $\pi/2 < \arg(\kappa_p) \leq 3\pi/2$  ( $p = 1, 2, 3$ ) are disregarded in the solutions. According to the method, the outer solution is valid everywhere outside the inner region. Assuming damping implies that the solutions should yield vanishing displacements when the axial variable  $s$  becomes infinite. This implies that the constant  $b_0$  must be set to zero. The six remaining constants appearing in the expressions of the inner and outer solutions have to be determined partly from the boundary conditions and partly from the matching conditions.

From equation (17), the boundary conditions satisfied by the leading term of the inner solutions are

$$(4m^4\tilde{w}_0 + \tilde{w}_0^{(4)})\mu^{-1}|_{\xi=0} = \tilde{n}_0, \quad \tilde{w}_0''|_{\xi=0} = \tilde{q}_0, \quad \tilde{w}_0''|_{\xi=0} = \tilde{m}_0. \quad (25)$$

By solving the system obtained when equation (22) are introduced into equation (25), the following results ensue:

$$C_{0,0}^1 = \mu\tilde{n}_0/4m^4, \quad C_{0,0}^2 = \frac{\tilde{m}_0}{2m^2(1+i)} + \frac{\tilde{q}_0}{4m^3}, \quad C_{0,0}^3 = \frac{i\tilde{m}_0}{2m^2(1+i)} + \frac{\tilde{q}_0}{4m^3}. \quad (26)$$

The matching of the outer and inner solutions is performed in the overlapping region, where the inner region variable  $\xi$  tends towards infinity and  $s$  tends towards zero. According to reference [17], the matching principle used to provide the missing equations is

$$\lim_{\xi \rightarrow +\infty} \tilde{w}_0(s; \lambda) = \lim_{s \rightarrow 0} \hat{w}_0(s; \lambda), \quad \lim_{\xi \rightarrow +\infty} \tilde{u}_0(s; \lambda) = \lim_{s \rightarrow 0} \hat{u}_0(s; \lambda). \quad (27)$$

Since the exponential terms in the inner solution describe a standing decaying wave, they might be taken as zero in this region. Furthermore, expressing the limits of the inner solutions in terms of the axial variable  $s$ , equation (27) become

$$C_{0,0}^1 + C_{0,1}^1 \frac{s}{\lambda} = d_0, \quad A_{0,0}^1 = -\frac{2m^2\sqrt{\Omega^2 - 1}}{\mu\Omega} d_0. \quad (28)$$

Inasmuch as the limit of the outer expansion does not contain a term proportional to  $\lambda^{-1}$ , the term  $\lambda^{-1}C_{0,1}^1$  in equation (28a) cannot be matched and the constant  $C_{0,1}^1$  should be taken to zero.

Finally, the analysis of the leading order is completed by deriving composite solutions which are valid both in the inner and the outer regions. According to Nayfeh [17], these composite expansions, denoted  $w^e$  and  $u^e$ , are defined by

$$w^e = w^o + w^i - \lim_{s \rightarrow 0} \hat{w}_0(s; \lambda), \quad u^e = u^o + u^i - \lim_{s \rightarrow 0} \hat{u}_0(s; \lambda). \quad (29)$$

Thus, using equations (18), (22), (24), (26), (28), (29) and (6) and the relationship  $D = \beta BR^2$ , the composite solutions, expressed as a function of the original load distributions, read, at the leading order,

$$w^e = \frac{\mu RN_0}{4m^4 B} e^{\kappa_1 s} + \frac{RQ_0}{4m^3 \beta^{1/4} B} (e^{\kappa_2 s} + e^{\kappa_3 s}) - \frac{M_0}{4m^2 \beta^{1/2} B} ((1-i)e^{\kappa_2 s} + (1+i)e^{\kappa_3 s}),$$

$$u^e = -\frac{R\sqrt{\Omega^2 - 1}}{2m^2 \Omega B} e^{\kappa_1 s}, \quad (30)$$



where the propagation constants are given by

$$\kappa_1 = -\frac{\Omega\sqrt{\Omega^2 - 1}}{2m^2}, \quad \kappa_{2,3} = \frac{-m(1 \pm i)}{\beta^{1/4}}. \quad (31a,b)$$

### 3.4. DISCUSSION

The first propagation constant given by equation (31a) describes a wave with a phase velocity close to the extensional phase speed in a beam at low frequencies and in a plate at high frequencies. This wave is referred to as the extensional wave in what follows. Likewise, the two remaining propagation constants given by equation (31b) tend toward the propagation constants of flexural wave in a flat plate at high frequencies. These waves are referred to as the flexural waves. From the expressions of the propagation constants, it appears that the vibration field can be described by two natural length scales, namely the  $l_1 = s/\beta^{1/4}$  and  $l_2 = s$ .

Upon considering equation (30), it is seen that the analysis of the leading order does not yield a complete wave receptance matrix. Indeed, the receptances of the extensional wave with respect to  $Q_0$  and  $M_0$  and the receptances of the flexural waves with respect to  $N_0$  do not appear at this stage. To derive the complete matrix, the analysis should be pursued to higher orders.

Finally, a second conclusion that can be drawn from equation (30) is that the approximate expressions become singular when the parameter  $m$  given by equation (3) vanishes, i.e., when the non-dimensional frequency  $\Omega$  tends towards  $\Omega_0 = \sqrt{1 - \mu^2}$ . These singularities do not appear in the real solutions and the problem of their treatment is tackled in section 5 by resorting again to perturbation theory.

## 4. THEORETICAL RESULTS

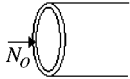
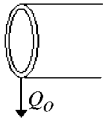
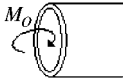
In this section, results issuing from the analysis of higher order solutions are given. The details of the calculations are not presented since the algebra, though becoming more cumbersome, is the same as in the preceding section. Yet a novelty appears for orders higher than 2 owing to the fact that equations (16) and (20) are no longer homogenous. The particular solutions of these non-homogeneous equations yield terms of the form  $s^p e^{\kappa s}$  in the composite solutions. For propagating waves, these terms, referred to as secular terms in perturbation theory [19], become unbounded as  $s \rightarrow \infty$ . Since the exact solution is bounded, the non-uniformities introduced by these terms should be removed. This can be achieved by using perturbation methods, e.g., the Lindstedt–Poincaré technique [19]. This method is based on the fact that these terms are nothing but the power-series expansion of the propagation constants. Upon realising that, it is then rather straightforward to make the solutions uniformly valid.

### 4.1. GREEN FUNCTIONS FOR THE RADIAL DISPLACEMENT

In order to obtain solutions for all the elements of the wave receptance matrices with respect to the radial displacement, the calculations are performed up to the fourth and to the second order in the case of the semi-infinite and infinite shells respectively. Table 1 provides the first non-zero term of the wave receptances for both problems as well as the order of magnitude of the first following term. From the knowledge of the wave receptances

TABLE 1

Wave receptances for the radial displacement;  $4m^4 = 1 - \mu^2 - \Omega^2$ ,  $\Theta = 1 - \Omega^2$  and  $\Psi = 1 - \mu\Omega^2/4m^4$

Excitation	Wave type	Semi-infinite shell (problem I)	Infinite shell (problem II)
	Extensional wave $p = 1$	$\alpha_{1,N_o}^{\infty/2} = \frac{\mu R}{4m^4 B} + O\left(\beta \frac{R}{B}\right)$	$\alpha_{1,N_o}^{\infty} = \frac{\mu R}{8m^4 B} + O\left(\beta \frac{R}{B}\right)$
	Flexural waves $\begin{cases} p = 2 \\ p = 3 \end{cases}$	$\alpha_{2,N_o}^{\infty/2} = -\beta^{1/2} \frac{(1-i)\Theta\Psi R}{16m^6 B} + O\left(\beta^{3/4} \frac{R}{B}\right)$	$\alpha_{2,N_o}^{\infty} = -\frac{\mu R}{16m^4 B} + O\left(\beta^{1/2} \frac{R}{B}\right)$
		$\alpha_{3,N_o}^{\infty/2} = -\beta^{1/2} \frac{(1+i)\Theta\Psi R}{16m^6 B} + O\left(\beta^{3/4} \frac{R}{B}\right)$	$\alpha_{3,N_o}^{\infty} = -\frac{\mu R}{16m^4 B} + O\left(\beta^{1/2} \frac{R}{B}\right)$
	Extensional wave $p = 1$	$\alpha_{1,Q_o}^{\infty/2} = -\beta^{3/4} \frac{\mu\Omega^2\Theta\Psi R}{32m^{11} B} + O\left(\beta^{7/4} \frac{R}{B}\right)$	$\alpha_{1,Q_o}^{\infty} = \frac{-i\mu^2\Omega R}{16m^6 B\sqrt{\Theta}} + O\left(\beta \frac{R}{B}\right)$
	Flexural waves $\begin{cases} p = 2 \\ p = 3 \end{cases}$	$\alpha_{2,Q_o}^{\infty/2} = \frac{R}{4m^3\beta^{1/4} B} + O\left(\beta^{1/4} \frac{R}{B}\right)$	$\alpha_{2,Q_o}^{\infty} = \frac{(1+i)R}{16m^3\beta^{1/4} B} + O\left(\beta^{1/4} \frac{R}{B}\right)$
		$\alpha_{3,Q_o}^{\infty/2} = \frac{R}{4m^3\beta^{1/4} B} + O\left(\beta^{1/4} \frac{R}{B}\right)$	$\alpha_{3,Q_o}^{\infty} = \frac{(1-i)R}{16m^3\beta^{1/4} B} + O\left(\beta^{1/4} \frac{R}{B}\right)$
	Extensional wave $p = 1$	$\alpha_{1,M_o}^{\infty/2} = \frac{\mu^2\Omega^2}{16m^8 B} + O\left(\beta^{1/2} \frac{R}{B}\right)$	$\alpha_{1,M_o}^{\infty} = \frac{\mu^2\Omega^2}{32m^8 B} + O\left(\beta \frac{R}{B}\right)$
	Flexural waves $\begin{cases} p = 2 \\ p = 3 \end{cases}$	$\alpha_{2,M_o}^{\infty/2} = -\frac{(1-i)}{4m^2\beta^{1/2} B} + O\left(\frac{R}{B}\right)$	$\alpha_{2,M_o}^{\infty} = \frac{i}{8m^2\beta^{1/2} B} + O\left(\frac{R}{B}\right)$
		$\alpha_{3,M_o}^{\infty/2} = -\frac{(1+i)}{4m^2\beta^{1/2} B} + O\left(\frac{R}{B}\right)$	$\alpha_{3,M_o}^{\infty} = \frac{i}{8m^2\beta^{1/2} B} + O\left(\frac{R}{B}\right)$

and by retaining the leading term of the propagation constants, it is straightforward to derive an approximate expression of the Green functions of the shell. These functions, given in general form by

$$G_X^c(x|0) = \alpha_{1,X}^c e^{\kappa_{1,X} x/R} + \alpha_{2,X}^c e^{\kappa_{2,X} x/R} + \alpha_{3,X}^c e^{\kappa_{3,X} x/R}, \quad (32)$$

describe the radial displacement of semi-infinite or infinite shells with respect to an axisymmetric load  $X$ . The wave receptances  $\alpha_{p,X}^c$  and the wave propagation constants  $\kappa_p$  are given in Table 1 and by equation (31) respectively.

In view of equation (31), three frequency domains can be distinguished depending on the nature of waves associated with the propagation constants. In domain I,  $\Omega < \sqrt{1 - \mu^2}$ , only the extensional wave is propagating while the flexural waves exhibit complex conjugate propagation constants characterizing a standing decaying field. In domain II ( $\sqrt{1 - \mu^2} < \Omega \leq 1$ ), the extensional wave and one of the flexural waves are purely evanescent while the second flexural wave is propagating. Finally, in domain III ( $\Omega > 1$ ), i.e., above the ring frequency, the extensional wave becomes propagating again and the flexural waves are both of the propagating and nearfield types.

#### 4.2. DIRECT MOBILITIES

Once the wave receptances are determined, the elements of the mobility matrix given by equation (12) are derived in accordance with equation (13) for both problems. The results are given in Table 2 where only the first non-zero terms for both the real and the imaginary parts of the mobilities are presented. In order to be able to trace the role played by the different waves, the contributions of the extensional wave to the mobilities have been underlined; the remaining terms are due to the flexural waves. For the semi-infinite shell, it proved necessary to carry on the analysis up to the seventh order in order to obtain the real part of the input mobility  $Y_{w,Q_0}^{\infty/2}$  for low frequencies.

#### 4.3. COMPARISON WITH "EXACT" RESULTS

Numerical solutions to problems I and II have been calculated according to the methodology described in section 2 by means of MATLAB<sup>®</sup> over the non-dimensional frequency range  $\Omega = 0.1-1.5$ . The physical properties of the shell used in the calculations are listed in Table 3. These "exact" solutions will serve in what follows as references with which the results from the approximate expressions will be compared.

Figure 2 shows the real part of the input mobilities for a semi-infinite shell. The anti-resonance exhibited by the real part of  $Y_{w,Q_0}^{\infty/2}$  at  $\Omega = \sqrt{1 - \mu}$  is due to the zero of the function  $\Psi$ . The agreement between "exact" and approximate solutions is very good for the whole frequency range, apart from at the resonance which occurs at  $\Omega_0 = \sqrt{1 - \mu^2}$ . As mentioned in section 3, this is the result of the singularities contained in the approximate solutions of Tables 1 and 2 when the parameter  $m$  vanishes. As shown later in section 5, the singularities can be removed and it is seen in Figure 2 that the new forms of solution given in Table 4, together with the values from Table 5 (both presented in section 5.1), are in good agreement with the exact calculations.

The error on the input radial force mobility introduced by the approximate expression has been assessed for the semi-infinite shell. Figure 3 shows the error versus frequency curves for three thickness-to-radius ratios. The ratio  $h/R$  was changed by keeping the radius  $R$  equal to  $R = 0.5$  m and varying the shell thickness accordingly. It is seen that the error is

TABLE 2

Direct mobilities for semi-infinite and infinite shells;  $4m^4 = 1 - \mu^2 - \Omega^2$ ,  $\Theta = 1 - \Omega^2$  and  $\Psi = 1 - \mu\Omega^2/4m^4$ ; the underlined terms represent the contributions of the extensional wave

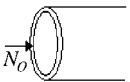
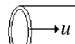
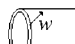

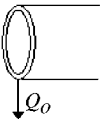
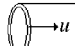
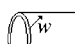

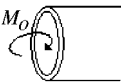
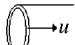
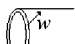

Excitation	Response	Semi-infinite shell (problem I)	Infinite shell (problem II)
	  	$Y_{u,N_o}^{\infty/2} = \frac{\omega R}{B} \left( \frac{\sqrt{\Theta}}{2m^2\Omega} + i\beta^{5/4} \frac{\Theta^2\Psi^2}{16m^9} \right)$ $Y_{w,N_o}^{\infty/2} = \frac{\omega R}{B} \left( \frac{i\mu}{4m^4} - \beta^{1/2} \frac{\Theta\Psi}{8m^6} \left( i + \beta^{1/4} \frac{\Omega\sqrt{\Theta}}{2m^3} \right) \right)$ $Y_{\theta,N_o}^{\infty/2} = \frac{\omega}{B} \left( \frac{\mu\Omega\sqrt{\Theta}}{8m^6} + i\beta^{1/4} \frac{\Theta\Psi}{4m^5} \right)$	$Y_{u,N_o}^{\infty} = \frac{\omega R}{B} \left( \frac{\sqrt{\Theta}}{4m^2\Omega} - \frac{i\mu^2\beta^{1/4}}{16m^5} \right)$ $Y_{w,N_o}^{\infty} = 0$ $Y_{\theta,N_o}^{\infty} = \frac{\omega}{B} \left( \frac{\mu\Omega\sqrt{\Theta}}{16m^6} + \frac{i\mu}{8m^3\beta^{1/4}} \right)$
	  	$Y_{u,Q_o}^{\infty/2} = Y_{w,N_o}^{\infty/2}$ $Y_{w,Q_o}^{\infty/2} = \frac{\omega R}{B} \left( \beta^{3/2} \frac{2\Omega^3\Theta^{5/2}\Psi^2}{256m^{16}} + \frac{i}{2m^2\beta^{1/4}} \right)$ $Y_{\theta,Q_o}^{\infty/2} = \frac{-\omega}{B} \left( \beta^{3/4} \frac{\mu\Omega^3\Theta^{3/2}\Psi}{64m^{13}} + \frac{i}{2m^2\beta^{1/2}} - \frac{i\mu}{4m^4} \right)$	$Y_{u,Q_o}^{\infty} = 0$ $Y_{w,Q_o}^{\infty} = \frac{\omega R}{B} \left( \frac{\mu^2\Omega}{16m^6\sqrt{\Theta}} + \frac{i}{8m^3\beta^{1/4}} \right)$ $Y_{\theta,Q_o}^{\infty} = 0$
	  	$Y_{u,M_o}^{\infty/2} = Y_{\theta,N_o}^{\infty/2}$ $Y_{w,M_o}^{\infty/2} = Y_{\theta,Q_o}^{\infty/2}$ $Y_{\theta,M_o}^{\infty/2} = \frac{\omega}{BR} \left( \frac{\mu^2\Omega^3\sqrt{\Theta}}{32m^{10}} + \frac{i}{m\beta^{3/4}} \right)$	$Y_{u,M_o}^{\infty} = Y_{\theta,N_o}^{\infty}$ $Y_{w,M_o}^{\infty} = 0$ $Y_{\theta,M_o}^{\infty} = \frac{\omega}{RB} \left( \frac{\mu^2\Omega^3\sqrt{\Theta}}{64m^{10}} + \frac{i}{4m\beta^{3/4}} \right)$

TABLE 3

*Physical properties of the shell*

Density, $\rho$ (kg/m <sup>3</sup> )	7800
Young's modulus, $E$ (N/m <sup>2</sup> )	$2.1 \times 10^{11}$
The Poisson ratio, $\mu$	0.3
Radius, $R$ (m)	0.5
Thickness-to-radius ratio, $h/R$	0.02

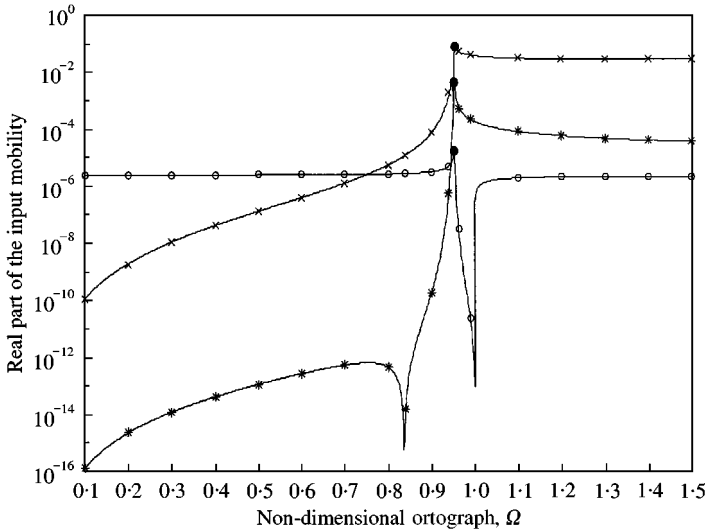


Figure 2. Real parts of the input mobilities for the semi-infinite shell. The lines indicate results obtained numerically with Flügge's theory while the symbols represent the values predicted by the expressions given in Table 2.  $\circ$ ,  $\text{Re}(Y_{u,N_0}^{\infty/2})$ ;  $*$ ,  $\text{Re}(Y_{w,Q_0}^{\infty/2})$ ;  $\times$ ,  $\text{Re}(Y_{\theta,M_0}^{\infty/2})$ . The "●" symbols at  $\Omega_0 = \sqrt{1 - \mu^2}$  are obtained by using results from section 5.

very small outside the resonance. Indeed, the error is lower than 1% outside the non-dimensional frequency region [0.92–0.97] for ratio  $h/R$  in the range [0.1–0.01]. Concerning the peak values at resonance, the simplified expressions derived in section 5 and given in Tables 4 and 5 yield a satisfying, even if poorer, agreement. These error values correspond to the modulus of  $Y_{w,Q_0}^{\infty/2}$  and can vary somehow between the results of Tables 1 and 2. A good estimate of the errors can be obtained by determining the first following term of the expansions for each quantities but this would involve very cumbersome algebra. As expected, it appears that the higher the thickness-to-radius ratio, the wider is the non-uniformity region where the solutions derived in section 3 break down. However, even for ratios  $h/R$  as high as 1/10, this region remains very narrow.

4.4. DISCUSSION

Upon considering the mobilities of the semi-infinite (problem I) and the infinite shell (problem II), respectively, it can be noticed that there is a factor 2 and 4 for the mobility parts due to the extensional wave and the flexural waves respectively. Therefore, the power flow injected by a bending moment, which in domain I is governed by the extensional wave,

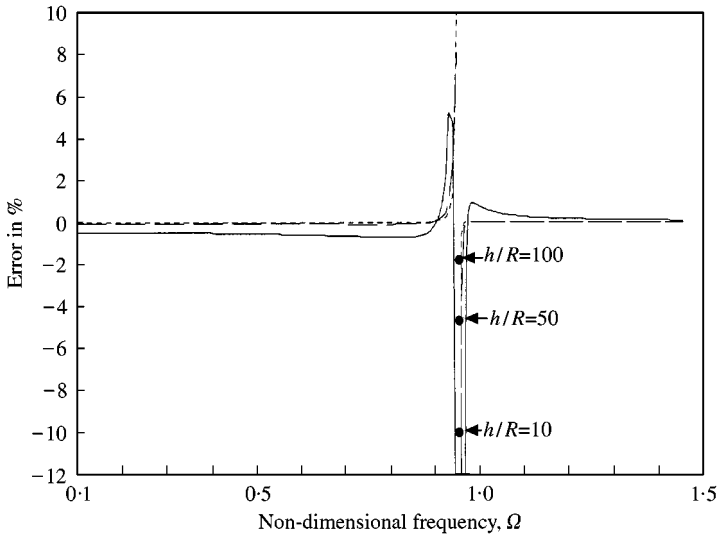


Figure 3. Error on the modulus of the input radial force mobility for the semi-infinite shell,  $|(Y_{w,Q_0}^{\infty/2})|$ . (—)  $h/R = 10$ , (---)  $h/R = 1/50$ , (- - -)  $h/R = 1/100$ . The “●” symbols at  $\Omega_0 = \sqrt{1 - \mu^2}$  are obtained by using results from section 5.

is doubled between problems I and II whereas the actual velocity at the excitation point, governed by the flexural waves, is 4 times greater. It also appears that for infinite structures, the real part of the mobilities is always related to the receptance of the propagating waves only and that these receptances are purely imaginary. For semi-infinite structures, waves of nearfield type can contribute to the real part of the mobilities as seen, for instance, in the case of the radial excitation. Indeed, for problem I, the receptances of the flexural waves are complex conjugate only for the first six orders but a difference occurs at  $k = 6$ . The contribution of the extensional wave to the injected power is due to the imaginary part of its receptance which arises at the order  $k = 11$ . Hence, the input power is injected via the flexural waves, the contribution of the extensional wave being negligible. Nevertheless, the great difference between the real parts of the input radial force mobility in problems I and II reveals that this process of injecting power via the non-propagating wave is not efficient.

Another point of interest that has arisen in the course of this study is the discrepancies in the analytical solutions resulting from the use of different shell theories. In respect to the boundary condition on the bending moment, moment per unit length is obtained by integrating the moments generated by the normal stresses  $\sigma_x$  shown in Figure 4 about the  $\phi$ -line and dividing by  $R d\phi$ . This yields

$$M_0 = \int_{-h/2}^{h/2} \sigma_x \left(1 + \frac{z}{R}\right) z dz. \quad (33)$$

Unlike in the case of the theory by Flügge [16], the term  $z/R$  is neglected in comparison to unity in the integrand in many theories, e.g., those by Love, Timoshenko, Donnell [14]. This simplification results in disregarding the contribution of the axial strain to moment resultant with respect to the effect of change of curvature of the midsurface. Therefore, the boundary conditions are given for these theories by

$$w''|_{s=0} = m_0, \quad w'''|_{s=0} = q_0, \quad (34)$$

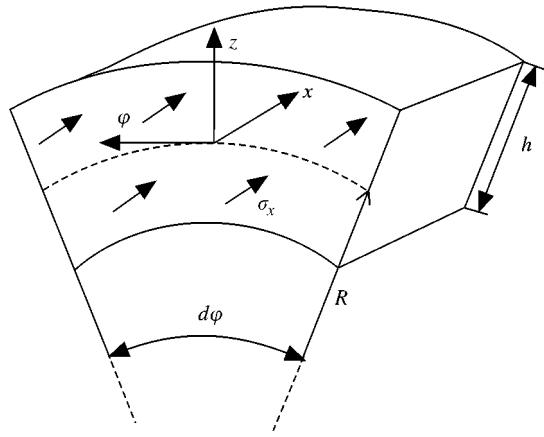


Figure 4. Normal stresses and shell section.

wherein the axial displacement is absent. Using these boundary conditions yields the same approximate expressions for the Green functions and the mobilities but with the function  $\Psi$  defined as  $\Psi = -\mu\Omega^2/4m^4$  instead of  $1 - \mu\Omega^2/4m^4$ . The effect of this change is significant below the ring frequency for problem I since  $\Psi$  appears in the expression of the real part of some mobilities. Solutions to the infinite shell problem are unaffected by such considerations.

Finally, considering the asymptotic behaviour of the approximate expressions at low or high frequencies yields some well-known results. For instance, the input impedance to the total axial force  $N$ , where  $N = 2\pi RN_0$ , acting on the shell extremity may be approximated at low frequencies ( $\Omega \ll 1$ ) by

$$Z = 1/Y_{u,2\pi RN_0}^{\infty/2} \approx \frac{\Omega B \sqrt{1 - \mu^2}}{\omega R} 2\pi R = \rho S c_L, \quad (35)$$

where  $S = 2\pi R h$  and  $c_L$  is the phase speed of extensional wave in a beam,  $c_L = \sqrt{E/\rho}$ . This result is similar to the input impedance of a beam of circular cross-section of radius  $R$  and thickness  $h$  excited at its end [3]. At high frequencies, the shell responds as a plate of thickness  $h$  submitted to a uniform axial load distribution  $N_0$ ,

$$Z = 1/Y_{u,N_0}^{\infty/2} \approx \Omega B / \omega R = \rho h c_{LI}, \quad (36)$$

where  $c_{LI}$  is the phase speed of extensional wave in a plate,  $c_{LI} = \sqrt{E/(\rho(1 - \mu^2))}$ .

Concerning the response to radial excitation at high frequencies ( $\Omega \gg 1$ ), the input impedance is given by

$$Z = 1/Y_{w,Q_0}^{\infty/2} \approx \frac{2B(-1)^{3/4}\Omega^{3/2}\beta^{1/4}}{4^{3/4}i\omega R} = 1/2\rho h c_B(1 + i), \quad (37)$$

where  $c_B$  is the phase speed of flexural wave in a plate,  $c_B = \sqrt{\omega} \sqrt[4]{Eh^2/(12\rho(1 - \mu^2))}$ . One can recognize the impedance of a flat plate to a uniform load distribution  $Q_0$  located at its edge. In fact, this impedance is the same as for a semi-infinite beam of unit width [3], with a minor correction on the bending wave speed to take into account the obstruction of the cross-sectional contraction in the circumferential direction. Finally, the fading of the leading term of the cross mobility  $Y_{w,N_0}^{\infty/2}$  reflects the uncoupling occurring at high frequencies between axial and radial displacements.

5. TREATMENT OF THE SINGULARITIES AT  $\Omega_0 = \sqrt{1 - \mu^2}$ 

As mentioned in section 3, the previous solutions become singular when  $m = 0$ , i.e., when  $\Omega = \Omega_0$ , and it can be seen in Tables 1 and 2 that the higher the order of the expansions terms, the greater the singularities. However, the singularities are not part of the actual solutions since exact calculations show that the resonance peaks exhibited by the shell vibrations in the vicinity of  $\Omega_0$  are of finite magnitude. The frequency region where the approximate solutions break down is referred to as the non-uniformity region. In spite of the narrowness of this region, the treatment of the singularities is of major importance due to the high vibration level undergone by the structure in this frequency range. Furthermore, for infinite shells excited by radial point force, Borgiotti *et al.* [8] have pointed out that the axisymmetric mode carries most of the power in this frequency region, the higher order circumferential modes being dominant at lower and higher frequencies.

## 5.1. WAVE RECEPTANCES FOR THE RADIAL DISPLACEMENT AND DIRECT MOBILITIES

To briefly outline the method used, the problem is re-formulated by using a row of variable changes. Then a perturbation analysis is performed with the thickness parameter as expansion parameter. Retaining only the leading term of the expansions yields forms of solutions which are considerably simplified with regard to the initial problem. For the detailed analysis of the treatment of the singularities, the reader is referred to Appendix A. The present section is devoted to the presentation of the results and their discussion.

As shown in Appendix A, the wave receptances and the direct mobilities can be represented by the formulae given in Table 4. These formulae contain the functions  $\check{\alpha}_{p,\check{X}}^c$ ,  $\check{Y}_{\check{u},\check{X}}^c$ ,  $\check{Y}_{\check{w},\check{X}}^c$  and  $\check{Y}_{\check{\theta},\check{X}}^c$  (with  $\check{X} = \check{n}_0, \check{q}_0, \check{m}_0$  and  $p = 1, 2, 3$ ) which are solely dependent upon the variable  $\gamma$  defined by

$$\gamma = \frac{(\Omega^2 - \Omega_0^2)}{\beta^{1/3} \mu^{4/3} \Omega_0^{4/3}}. \quad (38)$$

These functions should be computed, as they have no simple analytical expressions. For instance, the variations of the function  $\check{Y}_{\check{u},\check{n}_0}^{\infty/2}$  versus the variable  $\gamma$  are plotted in Figure 5. This curve represents the input axial force mobility made dimensionless by normalization with respect to  $\mu^{1/3} R \omega / \beta^{1/6} \Omega_0^{5/3} B$ . In Figure 5, are also shown mobilities values after identical normalization for the shell described in Table 3 and calculated with both Flügge's theory and the expression obtained in section 4 (see Table 2). It appears that  $\check{Y}_{\check{u},\check{n}_0}^{\infty/2}$  agrees nicely with the Flügge solution while the mobility given by Table 2 becomes singular at  $\gamma = 0$ .

Fortunately, owing to the sharpness of the resonance peaks and to their dependence upon  $\gamma$  only, there is no real need for an analytical description of  $\check{\alpha}_{p,\check{X}}^c$ ,  $\check{Y}_{\check{u},\check{X}}^c$ ,  $\check{Y}_{\check{w},\check{X}}^c$  and  $\check{Y}_{\check{\theta},\check{X}}^c$ . Instead, they can be described in terms of their most interesting characteristics. These characteristics, illustrated in Figure 5 for the function  $|\check{Y}_{\check{u},\check{n}_0}^{\infty/2}|$ , are denoted  $y_M$ ,  $\gamma_M$  and  $\Delta\gamma$ . They correspond to the peak values, the  $\gamma$ -values at which these peaks occur and the bandwidth of the resonance curve at  $y_M/\sqrt{2}$  respectively. They have been computed for all the functions and tabulated in Table 5 for the semi-infinite shell and in Table 6 for the infinite shell. Regarding the mobilities, characteristics are given for both the modulus and the real part of the functions since they are needed to assess the maximum displacement and



TABLE 4

Wave receptances and direct mobilities for semi-infinite and infinite shells at  $\Omega_0 = \sqrt{1 - \mu^2}$

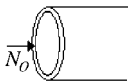
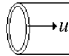
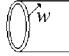

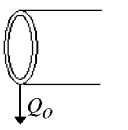
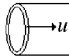
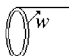

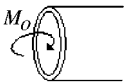
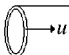
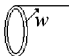

Excitation	Response	Wave receptance ( $p = 1, 2, 3$ )	Point mobility
		—	$Y_{u,N_0}^c = \frac{\omega R \mu^{1/3}}{\beta^{1/6} (1 - \mu^2)^{5/6} B} \check{Y}_{u,\check{n}_0}^c$
		$\alpha_{p,N_0}^c = \frac{R}{\beta^{1/3} \mu^{1/3} (1 - \mu^2)^{2/3} B} \check{\alpha}_{p,\check{n}_0}^c$	$Y_{w,N_0}^c = \frac{\omega R}{\beta^{1/3} \mu^{1/3} (1 - \mu^2)^{2/3} B} \check{Y}_{w,\check{n}_0}^c$
		—	$Y_{\theta,N_0}^c = \frac{\omega}{\beta^{1/2} (1 - \mu^2)^{1/2} B} \check{Y}_{\theta,\check{n}_0}^c$
		—	$Y_{u,Q_0}^c = Y_{w,N_0}^c$
		$\alpha_{p,Q_0}^c = \frac{R}{\beta^{1/2} \mu (1 - \mu^2)^{1/2} B} \check{\alpha}_{p,\check{q}_0}^c$	$Y_{w,Q_0}^c = \frac{\omega R}{\mu \beta^{1/2} (1 - \mu^2)^{1/2} B} \check{Y}_{w,\check{q}_0}^c$
		—	$Y_{\theta,Q_0}^c = \frac{\omega}{\mu^{2/3} \beta^{2/3} (1 - \mu^2)^{1/3} B} \check{Y}_{\theta,\check{q}_0}^c$
		—	$Y_{u,M_0}^c = Y_{\theta,N_0}^c$
		$\alpha_{p,M_0}^c = \frac{1}{\beta^{2/3} \mu^{2/3} (1 - \mu^2)^{1/3} B} \check{\alpha}_{p,\check{m}_0}^c$	$Y_{w,M_0}^c = Y_{\theta,Q_0}^c$
		—	$Y_{\theta,M_0}^c = \frac{\omega}{\beta^{5/6} \mu^{1/3} (1 - \mu^2)^{1/6} B R} \check{Y}_{\theta,\check{m}_0}^c$

TABLE 5

Characteristics of the resonance curves for the semi-infinite shell

	$\check{Y}_{u,\check{n}_0}^c$	$\check{Y}_{w,\check{n}_0}^c$	$\check{Y}_{\theta,\check{n}_0}^c$	$\check{Y}_{w,\check{q}_0}^c$	$\check{Y}_{\theta,\check{q}_0}^c$	$\check{Y}_{\theta,\check{m}_0}^c$	$\check{\alpha}_{1,\check{n}_0}^c$	$\check{\alpha}_{1,\check{q}_0}^c$	$\check{\alpha}_{1,\check{m}_0}^c$
<b>Modulus</b>									
$\gamma_M$	— 0.2	— 0.3	— 0.3	— 0.3	— 0.2	— 0.2	— 0.4	— 0.2	0.1
$y_M$	2.2	2.3	1.2	3.4	2.2	2.1	0.8	1.0	0.6
$\Delta\gamma$	1.0	1.0	0.9	1.0	1.0	1.6	1.8	1.0	2.3
	$\check{Y}_{u,\check{n}_0}^c$	$\check{Y}_{w,\check{n}_0}^c$	$\check{Y}_{\theta,\check{n}_0}^c$	$\check{Y}_{w,\check{q}_0}^c$	$\check{Y}_{\theta,\check{q}_0}^c$	$\check{Y}_{\theta,\check{m}_0}^c$			
<b>Real parts</b>									
$\gamma_M$	— 0.4	— 0.3	— 0.1	— 0.1	— 0.1	— 0.1	0.0	0.0	0.2
$y_M$	1.9	2.3	— 1.1	3.2	— 1.7	— 1.7	— 1.7	— 1.7	1.1
$\Delta\gamma$	0.8	0.6	0.6	0.7	0.7	0.7	0.9	0.9	2.9

the power input respectively. On the other hand, for the wave receptances, only the characteristics concerning the modulus of the receptance associated with the propagating wave are reported since they are sufficient to assess the vibration level in the far field.

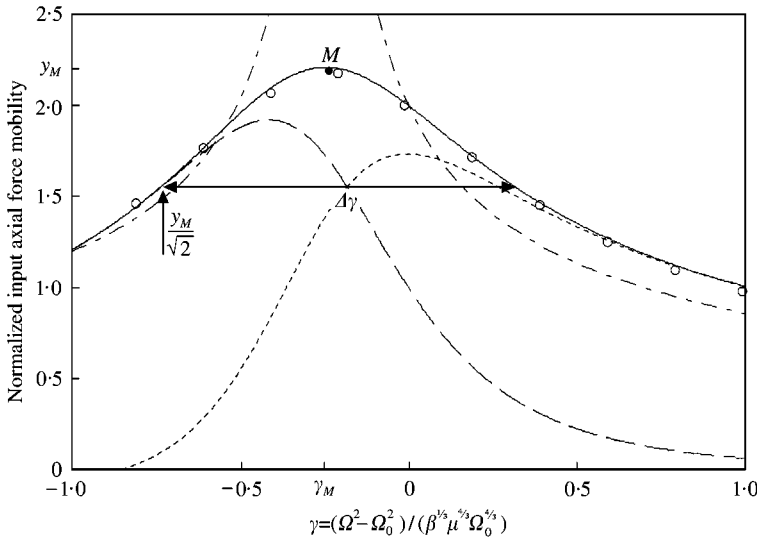


Figure 5. Input axial force mobility normalized with respect to  $\mu^{1/3}R\omega/\beta^{1/6}\Omega_0^{5/3}B$ . The “○” symbols and the dash-dot line, (— · —), represent the modulus of the “exact” solution from Flügge’s theory and of the predicted solution given in Table 2 respectively. (—)  $|\check{Y}_{\check{u},\check{n}_0}^c|$ , (— · —)  $\text{Re}(\check{Y}_{\check{u},\check{n}_0}^{c\alpha/2})$ , (---)  $-\text{Im}(\check{Y}_{\check{u},\check{n}_0}^{c\alpha/2})$ .

TABLE 6

*Characteristics of the resonance curves for the infinite shell*

	$\check{Y}_{\check{u},\check{n}_0}^c$	$\check{Y}_{\check{w},\check{n}_0}^c$	$\check{Y}_{\check{\theta},\check{n}_0}^c$	$\check{Y}_{\check{w},\check{q}_0}^c$	$\check{Y}_{\check{\theta},\check{q}_0}^c$	$\check{Y}_{\check{\theta},\check{m}_0}^c$	$\check{\alpha}_{1,\check{n}_0}^c$	$\check{\alpha}_{1,\check{q}_0}^c$	$\check{\alpha}_{1,\check{m}_0}^c$
<b>Modulus</b>									
$\gamma_M$	-0.9	/	-1.0	-1.0	/	-0.8	-1.2	-0.6	0.0
$y_M$	0.4	0	0.2	0.2	0	0.3	0.2	0.2	0.2
$\Delta\gamma$	6.0	/	4.8	4.7	/	9.0	3.4	3.4	5.0
<b>Real parts</b>									
$\gamma_M$	-1.9	/	-0.6	-0.6	/				1.1
$y_M$	0.28	0	0.2	0.2	0				0.2
$\Delta\gamma$	5.7	/	3.4	3.4	3.4	/			15.8

The analysis carried out in Appendix A also yields simplified forms for the propagation constants. They read

$$\kappa_p = (\mu^{1/3}\Omega_0^{1/3}/\beta^{1/6})\check{\kappa}_p, \tag{39}$$

where the constants  $\check{\kappa}_p$  are solutions of the dispersion relation

$$\check{\kappa}_p^6 - \gamma\check{\kappa}_p^2 + 1 = 0. \tag{40}$$

Figure 6 shows computed results for the propagation constants obtained with equation (40) (marked with the symbol “+”). The solid lines indicate the solutions of the “exact”

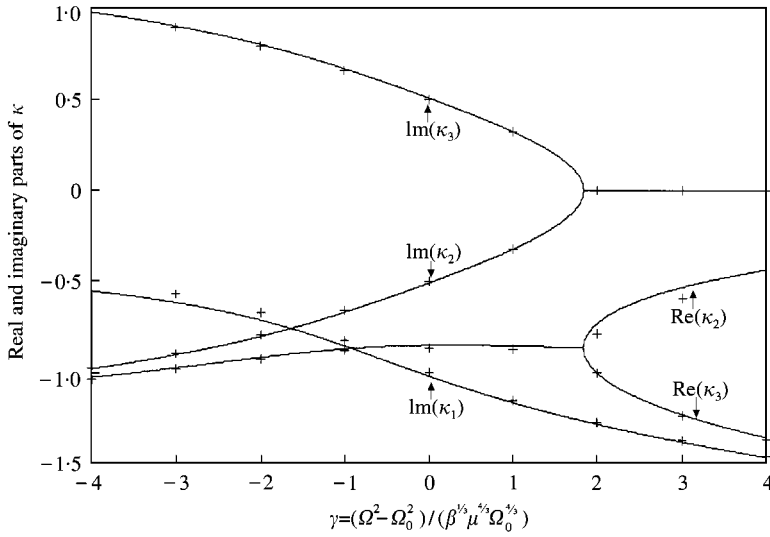


Figure 6. Real and imaginary parts of the propagation constants normalized with respect to  $\mu^{1/3}\Omega_0^{1/3}/\beta^{1/6}$ . (—) exact solutions calculated with Flügge theory, (+) solutions of equation (40).

dispersion relation from Flügge theory after normalization with respect to  $\mu^{1/3}\Omega_0^{1/3}/\beta^{1/6}$ . It is seen that the roots are either purely real or arise in complex conjugate pairs, the latter becoming real at  $\gamma = 3/\sqrt[3]{4}$ .

As shown in Figure 5, the non-dimensional frequency associated to the peak value is slightly shifted from  $\Omega_0$ . Using the values given in Tables 5 and 6 for  $\gamma_M$  together with equation (38), it is straightforward to obtain a better approximation of the “exact” resonance frequency  $\Omega_e$ . This yields

$$\Omega_e = \Omega_0 + \gamma_M \beta^{1/3} \mu^{4/3} \Omega_0^{1/3} / 2. \quad (41)$$

Finally, sharpness of resonance peaks can also be estimated using the values for  $\Delta\gamma$  provided by Tables 5 and 6. The current parameter used as a measure of sharpness is the quality factor  $Q$  defined by

$$Q = \Omega_e / \Delta\Omega_{1/\sqrt{2}}, \quad (42)$$

where  $\Delta\Omega_{1/\sqrt{2}}$  is the  $1/\sqrt{2}$ -value bandwidth. By using equations (38), (41) and (42), the quality factor can be approximated by

$$Q = 2(1 - \mu^2)^{1/3} / (\beta^{1/3} \mu^{4/3} \Delta\gamma). \quad (43)$$

As expected, equation (43) shows that the lower the shell thickness-to-radius ratio, the higher is the quality factor, namely the sharper is the resonance peak.

## 5.2. DISCUSSION

The analysis of the non-uniformity region reveals that, at the resonance, the vibration field is described by only one length scale ( $l_3 = s/\beta^{1/6}$ ), as shown by equation (39). Thus, the

axisymmetric radial-axial vibrations of shells involve three waves of the same nature in the vicinity of  $\Omega_0 = \sqrt{1 - \mu^2}$ . Furthermore, by comparing the values given in Tables 5 and 6, it appears that the magnitude and the quality factor of the resonance peaks for the semi-infinite shell are higher by a factor of 5 or more than those of the infinite shell.

Upon assuming damping in the shell material, its effect can be represented by introducing a complex modulus of elasticity, i.e., a complex non-dimensional frequency given by

$$\Omega^* = \left(1 - \frac{i\eta}{2}\right) \Omega, \quad (44)$$

where  $\eta$  is the loss factor. Replacing  $\Omega$  by  $\Omega^*$ , in the expression of the input mobility with respect to the axial force given in Table 2, i.e.,  $Y_{u,N_0}^{\infty/2}$ , the quality factor associated with the loss factor is approximately given by

$$Q = 1/\sqrt{3}\eta. \quad (45)$$

Upon equating equation (45) to equation (43), it appears that, if the loss factor is greater than the limit value given by

$$\eta_a = \beta^{1/3} \mu^{4/3} \Delta\gamma / 2\sqrt{3}(1 - \mu^2)^{1/3}, \quad (46)$$

the resonance is damping controlled. Below this value, it is the flexural rigidity which bounds the peak values. In practice, upon assuming the Poisson ratio of 0.3 and by taking  $\Delta\gamma = 2$  in view of Tables 5 and 6, the values of  $\eta_a$  are contained in the interval  $0.0025 \leq \eta_a \leq 0.012$  for values of  $h/R$  varying in the range  $1/10 \leq h/R \leq 1/100$ .

## 6. DERIVED RESULTS

### 6.1. REFLECTION COEFFICIENTS OF THE SHELL-BORNE WAVES AT A FREE END

Consider a semi-infinite shell lying in the half-space  $x \geq 0$  and a set of three negative-going waves of amplitude vector  $\mathbf{C}^- = [C_1^- \ C_2^- \ C_3^-]^T$  which is incident upon the free end of the shell at  $x = 0$ . These waves will give rise to reflected waves of amplitude vector  $\mathbf{C}^+ = [C_1^+ \ C_2^+ \ C_3^+]^T$  and the radial displacement  $w$  of the shell is given by

$$w = C_1^+ e^{\kappa_1 s} + C_2^+ e^{\kappa_2 s} + C_3^+ e^{\kappa_3 s} + C_1^- e^{-\kappa_1 s} + C_2^- e^{-\kappa_2 s} + C_3^- e^{-\kappa_3 s}. \quad (47)$$

The incident and reflected amplitude vectors are related by the reflection matrix  $\mathbf{r}$  for free termination defined by

$$\mathbf{C}^+ = \mathbf{r} \cdot \mathbf{C}^-. \quad (48)$$

The coefficient of the reflection matrix for the different types of waves can be derived from the knowledge of the wave receptances for the semi-infinite case. Consider a negative-going wave of type  $p$  incident upon the free end of the shell. This wave generates forces  $(N_0^*, Q_0^*, M_0^*)$  at  $x = 0$ . The amplitude of the reflected waves can then be assessed by using the Green function of the semi-infinite shell together with a load  $(-N_0^*, -Q_0^*, -M_0^*)$ . Hence, the vanishing of the loads at the extremity, i.e., the free end condition, is satisfied.

Applying this method to both the extensional and flexural waves yields the complete reflection matrix which reads at the leading order

$$\mathbf{r} = \begin{bmatrix} -1 & -(1-i)\beta \frac{\mu\Omega^2\Theta\Psi}{8m^8} & -(1+i)\beta \frac{\mu\Omega^2\Theta\Psi}{8m^8} \\ -i\beta^{3/4} \frac{\Omega\Theta^{3/2}\Psi}{4\mu m^5} & -i & 1+i \\ -i\beta^{3/4} \frac{\Omega\Theta^{3/2}\Psi}{4\mu m^5} & 1-i & i \end{bmatrix}, \quad (49)$$

where  $4m^4 = 1 - \mu^2 - \Omega^2$ ,  $\Theta = 1 - \Omega^2$  and  $\Psi = 1 - \mu\Omega^2/4m^4$ .

It appears that the coupling between the extensional and flexural waves, given by the element  $r_{12}$ ,  $r_{13}$ ,  $r_{21}$  and  $r_{31}$ , is very weak. Determined for the axial displacement, the element  $r_{11}$  is equal to 1, i.e., similar to the reflection coefficients for longitudinal wave in a rod [3]. The results derived here show that an extensional wave incident upon the free end of a shell does not yield radial displacement. Considering the reflection of flexural waves and their coupling, shows that the results are the same as for the flexural waves in a beam with free termination [20].

## 6.2. PROBLEM III: THE FINITE FREE-FREE SHELL

Consider a free-free cylindrical shell of length  $L$  excited at  $x = x_0$  by an axisymmetric load  $X$ , as shown in Figure 7. The mechanical response of the shell at frequencies below  $\Omega_0 = \sqrt{1 - \mu^2}$ , referred to as domain I, is deduced from the values of the wave receptances derived in problems I and II (see Table 1) and from the reflection matrix (see equation (49)). In domain I, only the extensional wave is propagating and the standing decaying field associated with the flexural waves vanishes much faster than the near field of bending wave in a beam. It can be noted that the lower the frequency, the greater is the decay. If the excitation is located outside the edge layer described in section 3, only the extensional wave reaches the edge. Furthermore, since it has been shown that the coupling between extensional and flexural waves is very small, the influence of the flexural waves can be assumed to be limited to a narrow region containing the excitation point and thus be disregarded at the shell extremities.

Following Cremer and Heckl [3], it is first assumed that the shell is infinite. The radial displacement produced by the load  $X$  and associated with the extensional wave is given by

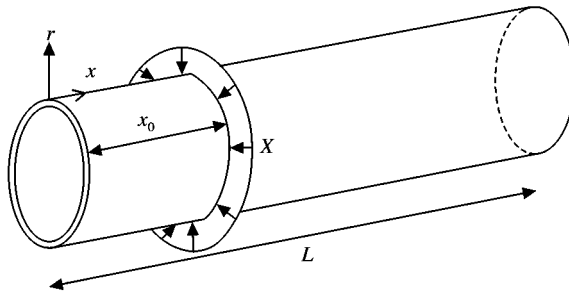


Figure 7. The finite free-free shell.

equation (32) and reads

$$w(x) = \begin{cases} \alpha_{1,X}^{\infty} e^{\kappa_1(x-x_0)/R} X & \text{for } x \geq x_0, \\ \alpha_{1,X}^{\infty} e^{-\kappa_1(x-x_0)/R} X & \text{for } x < x_0, \end{cases} \quad (50)$$

where  $\kappa_1$  is given by equation (31a) and the wave receptances  $\alpha_{1,X}^{\infty}$  by Table 1. Owing to the finite length of the shell, these waves will undergo an infinite series of reflections at the shell extremities characterized by a reflection coefficient of  $r_{11} = -1$ . It might be shown that the total vibration field generated by the extensional wave can be expressed as a sum of a geometric series, the characteristics of which are

$$U_0 = e^{\kappa_1 x/R} - e^{\kappa_1(2L-x)/R}, \quad q = e^{2\kappa_1 L/R}, \quad S(x) = \frac{e^{\kappa_1 x/R} - e^{\kappa_1(2L-x)/R}}{1 - e^{2\kappa_1 L/R}}, \quad (51)$$

where  $U_0$ ,  $q$  and  $S(x)$  are the first term, the common ratio and the sum of the geometric series respectively. Finally, it might be shown that the radial vibrations of the shell are described by

$$w(x) = 2i\alpha_{1,X}^{\infty} X \left\{ \sin(i\kappa_1 x_0/R) \frac{e^{\kappa_1 x/R} - e^{\kappa_1(2L-x)/R}}{1 - e^{2\kappa_1 L/R}} + H(x_0 - x) \sin(i\kappa_1(x - x_0)/R) \right\} \\ + \alpha_{2,X}^{\infty} X e^{\kappa_2|x-x_0|/R} + \alpha_{3,X}^{\infty} X e^{\kappa_3|x-x_0|/R}, \quad (52)$$

where  $H(x)$  is the Heaviside step function, i.e., is 0 for  $x < 0$  and 1 otherwise. The propagation constants and the wave receptances can be approximated by the expressions given in equation (31) and in Table 2 respectively. Finally, if the excitation is located at the edge, i.e.,  $x_0 = 0$ , the radial vibrations are given by

$$w(x) = \alpha_{1,X}^{\infty/2} \frac{e^{\kappa_1 x/R} - e^{\kappa_1(2L-x)/R}}{1 - e^{2\kappa_1 L/R}} X + \alpha_{2,X}^{\infty/2} X e^{\kappa_2 x/R} + \alpha_{3,X}^{\infty/2} X e^{\kappa_3 x/R}. \quad (53)$$

Equations (52) and (53) show that the shell response becomes infinite at the frequencies for which the denominator of the function  $S(x)$  vanishes. These frequencies correspond to the principle of wave cycle closure described in reference [3], i.e., the extensional wave closes on itself with the same phase after being reflected at both ends. Using equation (31a), these “natural” frequencies are the solutions of the equation

$$\frac{\Omega \sqrt{1 - \Omega^2}}{\sqrt{1 - \mu^2 - \Omega^2}} = \frac{n\pi R}{L} \quad \text{with } n = 1, 2, 3, \dots \quad (54)$$

Finally, the Green functions derived for the finite free–free cylindrical shell are compared to computed results obtained with the spectral finite element formulation developed by Finnveden [21] for straight fluid filled pipes. The comparison is made with a shell of length  $L = 20$  m excited by a harmonic radial load of magnitude  $Q_0 = 1$  N/m located at  $x = L/4$ . The other physical properties of the shell are listed in Table 3 and the non-dimensional frequency of the excitation is  $\Omega = 0.5$ . As shown in Figure 8, the radial displacement predicted by equation (52) is in good agreement with the numerical results obtained with the spectral finite element formulation.

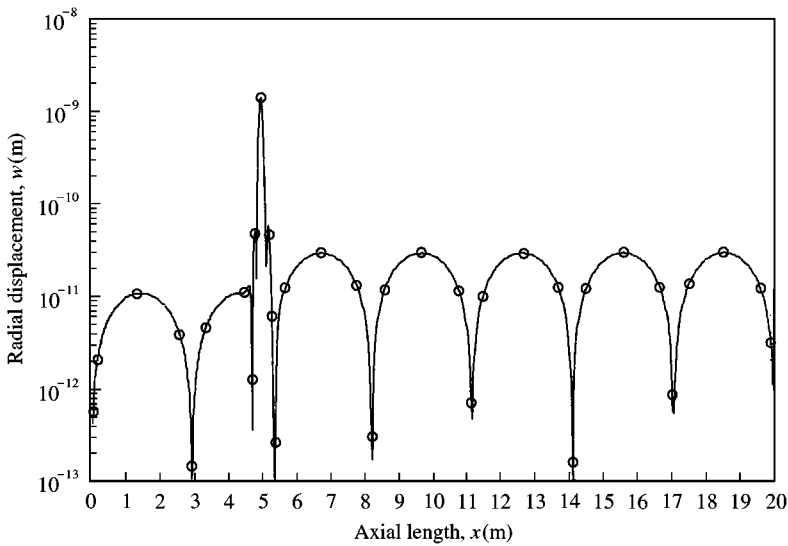


Figure 8. Shell response to a harmonic radial load applied at  $x = 5$  m. The non-dimensional frequency of the excitation is  $\Omega = 0.5$  and the load magnitude is  $Q_0 = 1$  N/m. The solid line represents the modulus of the radial displacement calculated numerically with the spectral finite element formulation [21]. The values predicted by equation (52) are marked with "O" symbols.

## 7. CONCLUSIONS

Perturbation techniques are applied to the analysis of the axisymmetric mode of vibration of cylindrical shells. It is shown that they yield accurate approximate expressions for the Green functions of semi-infinite or infinite shells with respect to force and moment excitation. By pursuing the analysis, it was also possible to derive closed form formulae for the mobilities of the shell with respect to axial and radial forces and a bending moment. The analysis reveals that the response of the shell at the excitation point could be determined by the flexural waves while the power flow injected within the structure is governed by the extensional wave. The present study also shows that differences in the closed form expressions arise in the case of the semi-infinite shell when different thin-walled shell theories are used to derive the real part of the input radial force mobility below the ring frequency. For the infinite shell, the approximate expressions remain the same, whatever the thin shell theory used for the derivation. Finally, the derived Green functions are used to determine approximate expressions for the reflection coefficients of the shell-borne waves at the free end and to study the axisymmetric vibrations of a finite free-free shell.

## ACKNOWLEDGMENTS

This work was supported by the Swedish National Energy Administration, which is gratefully acknowledged. I further would like to thank Professor S. Ljunggren, Professor J.-L. Guyader and Dr S. Finnveden for helpful discussions and comments.

## REFERENCES

1. J. E. MANNING *Philosophical Transactions of the Royal Society of London A* **346**, 477-488. Formulation of SEA parameters using mobility functions.

2. R. E. D. BISHOP and D. C. JOHNSON 1960 *The Mechanics of Vibration*. Cambridge: Cambridge University Press, 1979 re-issue.
3. L. CREMER, M. HECKL and E. E. UNGAR 1973 *Structure-Borne Sound*. Berlin: Springer-Verlag.
4. S. LJUNGGREN 1984 *Journal of Sound and Vibration* **93**, 161–187. Generation of waves in an elastic plate by a torsional moment and a horizontal force.
5. E. EICHLER 1964 *Journal of the Acoustical Society of America* **36**, 344–348. Plate-edge admittances.
6. C. KAUFFMANN 1998 *Journal of the Acoustical Society of America* **103**, 1874–1884. Input mobilities and power flows for edge-excited, semi-infinite plates.
7. J. L. PALLADINO and V. H. NEUBERT 1967 *Journal of the Acoustical Society of America* **42**, 403–411. Mobility of long cylindrical shell.
8. G. V. BORGIOTTI and E. M. ROSEN 1992 *Journal of the Acoustical Society of America* **91**, 911–925. The state vector approach to the wave and power flow analysis of the forced vibrations of a cylindrical shell. Part I: infinite cylinders in vacuum.
9. J. G. MCDANIEL 1998 *Journal of the Acoustical Society of America* **103**, 3386–3392. Power flow to a cylindrical shell with an attached structure.
10. R. S. MING, J. PAN and M. P. NORTON 1999 *Journal of the Acoustical Society of America* **105**, 1702–1713. The mobility functions and their application in calculating power flow in coupled cylindrical shells.
11. P. A. FRANKEN 1960 *Journal of the Acoustical Society of America* **3**, 473–477. Input impedances of simple cylindrical structures.
12. M. HECKL 1962 *Journal of the Acoustical Society of America* **34**, 1553–1557. Vibration of point-driven cylindrical shells.
13. J. G. SIMMONDS 1966 *Journal of Mathematics and Physics* **45**, 127–149. Influence coefficients for semi-infinite and infinite circular cylindrical shells.
14. A. W. LEISSA 1973 *Vibrations of Shells (NASA SO-288)*. Washington, DC: U.S. Government Printing Office.
15. S. K. WONG and W. B. BUSH 1993 *Journal of Sound and Vibration* **160**, 523–531. Axisymmetric vibrations of a clamped shell using matched asymptotic expansions.
16. W. FLÜGGE 1973 *Stresses in Shells*. Berlin: Springer-Verlag.
17. A. H. NAYFEH 1973 *Perturbation Methods*. New York: John Wiley & Sons, Inc.
18. A. H. NAYFEH 1985 *Problems in Perturbation*. New York: John Wiley & Sons, Inc.
19. J. A. MURDOCK 1991 *Perturbation: Theory and Methods*. New York: John Wiley & Sons, Inc.
20. B. R. MACE 1984 *Journal of Sound and Vibration* **97**, 237–246. Wave reflection and transmission in beams.
21. S. FINNVEDEN 1997 *Journal of Sound and Vibration* **199**, 125–154. Spectral finite element analysis of the vibration of straight fluid-filled pipes with flanges.

#### APPENDIX A: FORM OF THE SOLUTIONS IN THE NON-UNIFORMITY REGION

The singularities are dealt with by searching for approximate solutions valid in the region of non-uniformity. In perturbation theory [18], this problem is tackled by introducing a detuning parameter in the governing equations. In the present case, this parameter is taken as

$$\sigma = 4m^4/\beta^v, \quad (\text{A1})$$

where the constant  $v$  is a measure of the extent of the non-uniformity region. Additionally to equation (A1), a stretching transformation defined by

$$\xi = s/\beta^\varepsilon, \quad (\text{A2})$$

is introduced to derive a new variant of equation (2a). This yields

$$(1 - \beta)\beta^{1-6\varepsilon}w^{(6)} + \beta^{1-4\varepsilon}(\Omega^2 + 2\mu)w^{(4)} + \sigma\beta^{-2\varepsilon+v}w'' + \Omega^2(1 - \Omega^2)w + O(\beta) = 0. \quad (\text{A3})$$



The constants  $\varepsilon$  and  $\nu$  are determined by requiring that the first, third and fourth terms of equation (A3) are now of the same order of magnitude. It ensues that

$$\varepsilon = 1/6, \quad \nu = 1/3. \quad (\text{A4})$$

The following notation is then defined:

$$\tau = \beta^{1/6}, \quad \sigma = 4m^4/\beta^{1/3}, \quad (\text{A5})$$

together with the variables changes

$$\check{u} = -\frac{\Omega_0^{1/3}}{\tau\mu^{2/3}} u, \quad \check{w} = w, \quad \zeta = \frac{(\mu\Omega_0)^{1/3}}{\tau} s. \quad (\text{A6})$$

Introducing equations (A5) and (A6) into the governing equations (2) and omitting terms of order of magnitude  $O(\tau^2)$  or lower in the writing yields

$$\check{w}^{(6)} - \gamma\check{w}'' + \check{w} + O(\tau^2) = 0, \quad \check{u}' = \check{w} + O(\tau^2), \quad (\text{A7})$$

where the parameter  $\gamma$  is defined by

$$\gamma = -\sigma/(\mu\Omega_0)^{4/3}. \quad (\text{A8})$$

Similarly, when re-arranged with respect to equations (A5), (A6) and (A8), the boundary conditions (5) read

$$\begin{aligned} (\check{w}^{(4)} - \gamma\check{w} + O(\tau^2))|_{\zeta=0} &= \check{n}_0, & (\check{w}''' + O(\tau^2))|_{\zeta=0} &= \check{q}_0 \\ (\check{w}'' + O(\tau^2))|_{\zeta=0} &= \check{m}_0, \end{aligned} \quad (\text{A9})$$

where

$$\check{n}_0 = \frac{n_0}{\tau^2\mu^{1/3}\Omega_0^{4/3}}, \quad \check{q}_0 = \frac{\tau^3q_0}{\mu\Omega_0}, \quad \check{m}_0 = \frac{\tau^2m_0}{\mu^{2/3}\Omega_0^{2/3}}. \quad (\text{A10})$$

In the perturbation analysis, solutions are sought in the form of straightforward expansions given by

$$\begin{bmatrix} \check{u} \\ \check{w} \end{bmatrix} = \sum_{k=0}^{\infty} \tau^k \begin{bmatrix} \hat{u}_k \\ \hat{w}_k \end{bmatrix}. \quad (\text{A11})$$

Inserting equation (A11) into equation (A7) and collecting by terms of equal power of  $\tau$ , the leading term of the solution can be taken as

$$\hat{w}_0 = \sum_{p=1}^3 \check{C}_p e^{\check{\kappa}_p \zeta}, \quad \hat{u}_0 = \sum_{p=1}^3 \frac{\check{C}_p}{\check{\kappa}_p} e^{\check{\kappa}_p \zeta}, \quad (\text{A12})$$

where the constants  $\check{\kappa}_p$  are solutions of the dispersion relation

$$\check{\kappa}_p^6 - \gamma\check{\kappa}_p^2 + 1 = 0. \quad (\text{A13})$$

Thus, these constants have no simple analytical expressions except when  $\gamma = 0$  where they read  $(\check{\kappa}_1, \check{\kappa}_2, \check{\kappa}_3) = (-i, e^{5i\pi/6}, e^{7i\pi/6})$ .

The amplitudes of the waves  $\check{C}_p$  in equation (A12) are related to the loads  $\check{X}$  given by equation (A10) by the wave receptance matrix  $\check{\alpha}^c$  defined by

$$[\check{C}_1 \quad \check{C}_2 \quad \check{C}_3]^T = \check{\alpha}^c [\check{n}_0 \quad \check{q}_0 \quad \check{m}_0]^T, \quad (\text{A14})$$

where the superscript  $c$  indicates if reference is made to problem I or II. The elements of this matrix,  $\check{\alpha}_{p,\check{X}}^c$  are determined by inverting the system obtained when equation (A12) is introduced in the boundary condition (A9). The expressions of these coefficients are very cumbersome since they contain the roots of equation (A13). By using equations (A10)–(A12), (A6), (A14) and (6), the receptances of the waves are expressed in terms of the original variables and read

$$\begin{aligned} \alpha_{p,N_0}^c &= \frac{R}{\beta^{1/3} \mu^{1/3} \Omega_0^{4/3} B} \check{\alpha}_{p,\check{n}_0}^c, & \alpha_{p,Q_0}^c &= \frac{R}{\beta^{1/2} \mu \Omega_0 B} \check{\alpha}_{p,\check{q}_0}^c, \\ \alpha_{p,M_0}^c &= \frac{1}{\beta^{2/3} \mu^{2/3} \Omega_0^{2/3} B} \check{\alpha}_{p,\check{m}_0}^c. \end{aligned} \quad (\text{A15})$$

Likewise, using equations (13) and (A15) for the derivation of the mobilities yields the expressions

$$\begin{aligned} Y_{u,N_0}^c &= \frac{\omega R \mu^{1/3}}{\beta^{1/6} \Omega_0^{5/3} B} \check{Y}_{\check{u},\check{n}_0}^c, & Y_{w,N_0}^c &= \frac{\omega R}{\beta^{1/3} \mu^{1/3} \Omega_0^{4/3} B} \check{Y}_{\check{w},\check{n}_0}^c, & Y_{\theta,N_0}^c &= \frac{\omega}{\beta^{1/2} \Omega_0 B} \check{Y}_{\check{\theta},\check{n}_0}^c, \\ Y_{w,Q_0}^c &= \frac{\omega R}{\mu \beta^{1/2} \Omega_0 B} \check{Y}_{\check{w},\check{q}_0}^c, & Y_{\theta,Q_0}^c &= \frac{\omega}{\mu^{2/3} \beta^{2/3} \Omega_0^{2/3} B} \check{Y}_{\check{\theta},\check{q}_0}^c, \\ Y_{\theta,M_0}^c &= \frac{\omega}{\beta^{5/6} \mu^{1/3} \Omega_0^{1/3} B R} \check{Y}_{\check{\theta},\check{m}_0}^c, \end{aligned} \quad (\text{A15})$$

where the functions  $\check{Y}_{\check{u},\check{X}}^c$ ,  $\check{Y}_{\check{w},\check{X}}^c$  and  $\check{Y}_{\check{\theta},\check{X}}^c$  are given by

$$\check{Y}_{\check{u},\check{X}}^c = i \sum_{p=1}^3 \frac{\check{\alpha}_{p,\check{X}}^c}{\check{K}_p}, \quad \check{Y}_{\check{w},\check{X}}^c = i \sum_{p=1}^3 \check{\alpha}_{p,\check{X}}^c, \quad \check{Y}_{\check{\theta},\check{X}}^c = i \sum_{p=1}^3 \check{\alpha}_{p,\check{X}}^c \check{K}_p. \quad (\text{A16})$$

Considering equations (A13), (A9), (A12) and (A16) indicates that the coefficients  $\check{K}_p$ ,  $\check{\alpha}_{p,\check{X}}^c$ ,  $\check{Y}_{\check{u},\check{X}}^c$ ,  $\check{Y}_{\check{w},\check{X}}^c$  and  $\check{Y}_{\check{\theta},\check{X}}^c$  are solely function of the parameter  $\gamma$  defined in equation (A8).

## APPENDIX B: NOMENCLATURE

$A$	wave amplitude in the axial direction
$B$	extensional rigidity ( $Eh/(1 - \mu^2)$ )
$C$	wave amplitude in the radial direction
$D$	flexural rigidity ( $\beta BR^2$ )
$E$	Young's modulus
$G$	Green function for the radial displacement
$H$	Heaviside step function
$L$	shell length
$M_0$	bending moment per unit length in the $r, x$ plane
$N_0$	axial force per unit length
$Q$	resonance quality factor
$Q_0$	radial force per unit length
$R$	shell radius

$T$	wave amplitude ratio ( $A/C$ )
$Y$	direct mobility
$\mathbf{Y}^c$	mobility matrix
$Z$	impedance
$c$	superscript; $\infty/2$ and $\infty$ for the semi-infinite and infinite shell respectively
$h$	shell thickness
$i$	$\sqrt{-1}$
$m$	parameter defined by $4m^4 = 1 - \mu^2 - \Omega^2$
$r$	cylindrical co-ordinate
$\mathbf{r}$	reflection matrix
$s$	non-dimensional axial length ( $x/R$ )
$t$	time
$u$	midsurface displacement in the $x$ direction
$v$	midsurface displacement in the $\varphi$ direction
$w$	midsurface displacement in the $r$ direction
$x$	cylindrical co-ordinate
$\boldsymbol{\alpha}^c$	wave receptance matrix
$\alpha_{p,x}^c$	receptance of the wave $p$ with respect to the load $X$
$\beta$	thickness parameter ( $h^2/(12R^2)$ )
$\delta$	Kronecker's delta function ( $\delta(k, 0) = 1$ if $k = 0$ , 0 otherwise)
$\eta$	shell loss factor
$\theta$	rotation of the normal to the middle surface about the $\varphi$ -axis ( $\partial w/\partial x$ )
$\varphi$	cylindrical co-ordinate
$\kappa$	non-dimensional propagation constant
$\lambda$	expansion parameter
$\mu$	the Poisson ratio
$\xi$	inner region axial length
$\rho$	density of the shell material
$\omega$	circular frequency of the excitation
$\Omega$	non-dimensional frequency ( $\omega R \sqrt{\rho(1 - \mu^2)/E}$ )
$(\dot{\quad})$	differential with respect to time
$ z $	modulus of the complex number $z$